

## Original Article

# Changes in and effects of Kupffer cells on residual tumor after cryoablation in rabbit hepatic VX2 tumor

Fengtao Yi\*, Lei Liu\*, Menglan Ding\*, Yaling Zhu, Qingling Song, Ceng Zeng

Department of Oncology, General Hospital of Central Theater Command of Chinese People's Liberation Army, No. 627 Wuluo Road, Wuchang District, Wuhan 430070, Hubei, P. R. China. \*Equal contributors.

Received July 28, 2020; Accepted November 12, 2020; Epub January 1, 2021; Published January 15, 2021

**Abstract:** Objective: Cryoablation can directly kill tumor cells through sudden changes in temperature. It can also enhance lymphocyte function and cause distant tumor regression far from the ablation treatment area. In order to further explore the changes of immune function after cryoablation, the changes of Kupffer cells (KCs), the main immune cells in the liver, and their effects on untreated tumors *in vivo* were studied. Methods: Rabbit VX2 liver cancer models were constructed. The growth of liver tumors was confirmed by ultrasound after transplantation for 3 weeks. Fifteen Japanese white rabbits were divided into a tumor control group and cryoablation group. Cryoablation group was treated with cryoablation of a single or partial tumor. Histologic and immunohistochemical changes of the treatment area and untreated tumor area before and after cryoablation were observed, and the phagocytic function changes of KCs around the untreated area and treatment area were observed by electron microscopy. Results: Cryoablation areas showed necrosis, infiltration of inflammatory cells (including KCs), and fibrosis of tissue. The number of inflammatory cells in the unfrozen tumor area was increased in the same treated rabbit. There was a significant difference in the maximum diameter of unfrozen tumors between the frozen group and control group at 15th days after cryoablation ( $P < 0.05$ ), while the difference was not obvious at the 3rd and 7th day ( $P > 0.05$ ). Electron microscopy showed that the number of debris fragments engulfed by KCs around the tumor after cryoablation was significantly higher than that of the control group. In the same rabbit, we compared the amount of debris between tissue surrounding the unfrozen area and around the cryoablation area. There was a significant difference on the 3rd day after cryoablation,  $P = 0.043$ , while there was no significant difference on the 7th day,  $P = 0.348$ . Conclusion: After cryoablation, inflammatory cells aggregated around the cryoablated area. The activity of KCs had been increased and the function of phagocytosis enhanced. KCs had a certain inhibitory effect on the untreated tumor in the same animal at the early stage (within 15 days), but it was not enough to restrain the growth of the untreated tumors.

**Keywords:** Cryoablation, Kupffer cells, immune function, rabbit hepatic VX2 tumor

## Introduction

Liver cancer is one of the most common malignancies, with the third highest cancer-related mortality worldwide, and the incidence rate is about 25.7/10 million. Unfortunately, there were 0.745 million patients with liver cancer who died [1, 2]. The five-year survival rate of patients after curative resection of hepatocellular carcinoma (HCC) has been reported to be 30% to 50%, but the actual survival rate may be higher. Half the patients had recurrence, with a majority occurring within one year (65%). These patients with early recurrence had a poor actual 5-year survival rate of 5% [3, 4]. In the mid-1850s, cryotherapy was applied to the

treatment of tumors, and could relieve pain and diminish the mass [5]. Argon-helium cryoablation is a physiotherapy technique developed in the past 20 years. Compared to other topical treatment methods in liver cancer treatment such as percutaneous ethanol injection (PEI), laser and microwave coagulation, radiofrequency hyperthermia, or high intensity focused ultrasound therapy, it has many features such as obvious boundaries, easy to monitor treatment area, and uniform tissue destruction, and it is available to monitor the entire process [6]. Previously, its main therapeutic principle was to directly kill tumor cells through sudden changes in temperature. In recent years, some reports described that cryoablation could result

## Effect of Kupffer cells on residual tumor after cryoablation

in T lymphocyte function enhancement, and tumors distant from the ablation treatment area also showed a regressive tendency after ablation treatment, which indicated that the immunologic function had changed after ablation treatment [7, 8]. However, as a physical therapy, cryoablation has not been reported in the mechanism of induction of immune function changes, especially regarding its conditioning effect on immune function. This study explores expression and phagocytosis changes of Kupffer cells (KCs) in the tissues adjacent to the cryoablated area when the liver tumor was treated with cryoablation.

Macrophages are the first line of host defense against pathogens, and interest in their function and ontogeny has since grown tremendously [9]. They represent a key cellular component of the liver. They are essential for maintaining tissue homeostasis and ensuring rapid responses to hepatic injury [10]. Liver macrophages are attracting interest due to their crucial roles in homeostasis and hepatic diseases. KCs, a specific macrophages in the liver, also known as stellate macrophages and Kupffer-Browicz cells, are the largest intrinsic macrophage group in the human body, accounting for about 80-90% of the total number of intrinsic macrophages. They have all the characteristics of macrophages [11, 12]. They form part of the mononuclear phagocyte system. KCs are large in size and irregular in morphology, and have many pseudopodia on the surface. They mainly adhere to endothelial cells, or penetrate through the apertures and enter into the perisinusoidal space, and are in direct contact with hepatocytes and hepatic stellate cells [13]. They engulf the antigen-antibody complexes from blood circulation, damaged and necrotic hepatocytes, and other harmful substances. They function as a non-specific immune cell by eliminating the damage by these substances to the body. Simultaneously, KCs participate in the inflammatory response at the injured site through its secretory action, and play an active role in tumor immunity. The active role in the body is an important part of the body's immune function [14].

The aim of this study was to investigate the changes of KCs around frozen tumors and unfrozen tumors after cryoablation in rabbit liver VX2 tumors. We explored the changes in

tumor size, and the effects of immune function changes.

### Materials and methods

#### *Animals, main reagents, equipment and sources*

Japanese male white rabbits were purchased from Center for Animal Experiment of Wuhan University; VX2 tumor cell lines were purchased from the cell storage center of Wuhan University. Sumianxin II Injection (anesthetic agent) was purchased from the Research Institute of Veterinary Medicine, Changchun Academy of Military Medical Sciences (lot No. 07003). Fluorescence microscopy was manufactured by Zeiss Corporation; ordinary microscopy was manufactured by Olympus Corporation. Dry thermostat was manufactured by Hangzhou Allsheng Instruments Co., Ltd. Water bath kettle was produced by Jiangnan Instrument Factory of Jintan City. Argon-Helium knife was manufactured by ENDOCARE Corporation of the United States. H-7000 transmission electron microscopy was produced by Japan Hitachi Electric Co., Ltd.

#### *Experimental methods*

*Animal anesthetization:* According to the method in the previous article [15], 18 Japanese male white rabbits, with the age from 5 to 8 months and weight from 3 kg to 5 kg were anesthetized with Sumianxin II Injection, dose of 0.1 ml/kg, in intramuscular injection. After 5 minutes, the anesthetic effect was achieved: a drowsy state, with no apparent response to surgical stimulation.

*Rabbits VX2 liver cancer model construction:* The tumor-bearing rabbits with VX2 tumor were anesthetized and supine. The head and limbs were fixed on the operating table dedicated to rabbit experiments. The surgical site (tumor growth site, located in the liver) was depilated, disinfected, and covered with an aseptic hole-towel. We incised the skin, exposed and removed the tumor, got rid of the surrounding adipose tissue and normal liver tissue, cut open the tumor with a surgical blade, and scraped away the necrotic tissue, leaving a shiny white fish-like and well-growth tissue. This was put into normal saline with an appropriate amount of calf serum added, and cut

## Effect of Kupffer cells on residual tumor after cryoablation

into small pieces less than 1 mm in diameter for spare. After a healthy Japanese white rabbit being anesthetized, the head and limbs were fixed on an operating table dedicated to rabbit experiments. The abdomen was shaved and the abdomen skin was dissected to expose a small amount of liver. The tumor tissue was implanted into left and right lobes with the ophthalmologic smooth forceps, 1.5 cm from the edge of the liver. The implant hole was filled with sterile gelatin sponge, and then the abdominal cavity was sutured. We prevent infection with 0.5 g of cefazolin sodium (Shandong Lukang Pharmaceutical Co. LTD, lot No. H20131691), in intramuscular injection. We detected intrahepatic tumor growth with ultrasonography at the 3rd week after intrahepatic VX2 tumor cell line transplantation. Fifteen tumor-bearing rabbits with the appropriate tumor sizes were selected for the experiment in all rabbits (tumor size was 0.5-2.1 cm, number of tumors was about 1-4, all located in the liver) [16, 17].

*Grouping and cryotherapy:* Tumor-bearing white rabbits were randomly divided into 5 groups, 3 in each group. They were: the control group (pre-cryoablation group), the 3-day cryoablation group, the 7-day group, the 15-day group, and the 30-day group. The tumor-bearing white rabbits were fixed on the animal experiment table. The abdomen was depilated, disinfected, covered with an aseptic hole-towel. We incised the skin and peritoneum, and exposed the liver to observe and record the number, size, and shape of the tumors inside according to the method in the previous article [18, 19]. A 2 mm ultra-cold knife was then inserted from the middle of the tumor and passed through the tumor approximately 0.2 cm. After being inserted into place, normal temperature and high pressure argon gas was put through to perform cryoablation. The temperature of knife tip dropped to  $-135^{\circ}\text{C}$  within 30 seconds. The input power was controlled to ensure that an ice ball covered the tumor and lasted 10 to 20 minutes. Then we stopped argon gas infusion. We changed to infuse the high pressure helium gas at normal temperature. The temperature of the knife tip rose to  $20^{\circ}\text{C}$  in 3 minutes, with ice ball melting visible, and then freezing-rewarming cycle was done once. We removed the superconducting knife, filled with the gelatin sponge to stop bleeding, disinfected and

sutured the skin. We prevent infection with 0.5 g of cefazolin sodium, by intramuscular injection.

*Processing:* 3 rabbits were executed before cryoablation and on the 3rd day, 7th day, 15th day and 30th day respectively after cryoablation. The livers were removed and the color, number, size, and shape of the tumors were observed and recorded. After electron microscopy samples were taken, the tumors were broken open and placed in 40% formaldehyde solution (Jinan Dahui Chemical Co. LTD, lot No. 20131005) to fix, routinely paraffin embedded, and received H&E staining and immunohistochemical staining.

*H&E staining:* According to the method in the previous article [20], paraffin sections were dehydrated to transparency, stained, and mounted and observed under a microscopy.

*SP immunohistochemical staining:* According to the method in a previous article [21, 22], paraffin sections were routinely deparaffinized to water and incubated with 3% hydrogen peroxide solution (Aladdin, H299581) for 10 minutes to block endogenous peroxidase activity. After washing with PBS solution (Hyclone, lot No. AD16192277) several times, the sections were immersed in a 0.01 M sodium citrate buffer solution (LABEST, PM5100-10) and heated to boiling by a microwave oven and then powered off. The slices were placed in a plastic slice holder and immersed in a buffer solution. The sample was heated in a low fire for 8 minutes. The buffer pocket was soaked in cold water and allowed to cool, which was repeated 3 times. After cooling, it was washed with PBS for 3 min, repeated 3 times. After the PBS was discarded, normal goat serum (Beyotime, C0265) blocking reagent was dropwise added, sealed and incubated at  $37^{\circ}\text{C}$  for 20 minutes. Excess antibodies were drained and not washed. An anti-rabbit macrophage (CD68) monoclonal antibody (1:200 dilution) (Beyotime, AF2320) was added dropwise and placed in a humid chamber overnight at  $4^{\circ}\text{C}$ . After rewarming at room temperature for 30 minutes, it was washed with PBS solution for 5 min, repeated 4 times. Excess liquid was absorbed, and we added biotin-labeled secondary antibody (Beyotime, P0628) and incubated at  $37^{\circ}\text{C}$  for 20 minutes. We washed with PBS solution several times and added reagent SABC (Beyotime,

## Effect of Kupffer cells on residual tumor after cryoablation

P0628) to incubate at 37°C for 20 minutes. After washing, we did DAB (Solarbio, DA1015) staining, after about 3-5 min, washed with tap water to stop the color reaction; did hematoxylin staining (Solarbio, H8070) for 2 min, and washed with tap water. Slides were soaked in hydrochloric-alcohol solution rapidly, wash again, soaked in ammonia solution, washed with tap water, and then observed under microscopy. We dehydrated step by step, gradually mounted with neutral balsam, and observed and collected the images under microscopy.

**Electron microscopy detection [23]:** ① The liver lobe was inoculated with VX2 tumor cells and treated with cryoablation and another liver lobe (2 lobes in total) was inoculated with VX2 tumor cells but without cryoablation. These were obtained separately and 2 parts of each lobe were taken. The one part was placed into formaldehyde fixative solution for light microscopy sample preparation. The other part was placed in 2.5% glutaraldehyde (MERCK, G5882) for electron microscopy sample preparation; ② Electron microscopy for secondary sample preparation: the hepatic tissue between hepatic portal area and lesion was cut. A small piece of 1\*1\*2 mm was collected and fixed with 2.5% glutaraldehyde for 2 hours, and washed with PBS for 3 times, 10 minutes/time. ③ After that, it was fixed 1% osmic acid (AIKE REAGENT, 20816-12-0) for 1 hour and washed with PBS for 3 times, 10 minutes/time; ④ Then it was dehydrated with 50%, 70%, 80%, 90%, 95%, and 100% acetone, 10 minutes per solution; ⑤ Acetone: EPON 812 resin (Beijing Jiehuibo Biotechnology Co. LTD, 2311S) = 1:1 was used to soak for 12 hours in 37 degrees incubator; Pure EPON 812 resin was used to soak for 12 hours in 37 degrees incubator; ⑥ Polymerization was kept for 48 hours in a 60 degree incubator; ⑦ Ultrathin sectioning was conducted in Leica ultramicrotome, with the thickness of 50-60 nm. We removed and deposited the sections on copper mesh (200 mesh) with Formvar membrane; ⑧ Uranyl acetate (Shanghai Rongbai Biotechnology Co. LTD, rbr00588) and lead citrate (Shanghai Yiji Industrial Co., LTD, YJ-512265) were used for double staining; ⑨ We observed and collect images under Hitachi H-7000 transmission electron microscopy.

### Statistical analysis

Statistical analyses were performed using SPSS19.0 (Version X; IBM, Armonk, NY, USA)

[24]. Count data were expressed as mean  $\pm$  standard deviation ( $\bar{x} \pm s$ ), using T-test and analysis of variance. The test level was considered significant at  $P < 0.05$ .

### Results

#### *Unfrozen tumor in the frozen group grew slower on the 15th day after cryoablation*

Only the right lobe tumor of each white rabbit had been treated with cryoablation, and the remaining tumor served as its own control. Changes in the size of unfrozen tumors in the control group and frozen group revealed that there was no significant difference on the 3rd and 7th day after cryoablation ( $P > 0.05$ ) (**Figure 1A, 1B**). On the 15th day after cryoablation, there was an obvious increase around the unfrozen tumors of the control group and frozen group, and the difference was significant ( $P < 0.05$ ) (**Figure 1C**).

#### *Comparison of the appearance and histology of the tumors before and after cryoablation*

Before cryoablation, the tumors were nodular and smooth in surface and had no capsule formation, and the boundary between the liver and the surrounding liver tissue was unclear, fish-meat like appearance. There was necrosis in tumors more than 0.5 cm, milky residue-like material. After 3rd day of cryoablation, the frozen area showed a circular necrotic area. The inner cells of the tumor were swollen. Nuclear fragmentation was seen and the cell structure was incomplete. Inflammatory cells were observed by H&E staining between the normal liver tissue and the tumor necrotic tissue that were small like a nucleus. If the treatment area of tumor was not completely covered by an ice ball, the tumor cells could be seen around the area. Meanwhile, the anti-CD68 immunohistochemical staining was strongly positive and showed that many inflammatory cells were scattered among the unfrozen tumor cells. On the 7th day after cryoablation, the frozen area was grayish and there was no luster on the surface of necrotic area with clear boundary. There were no intact cells in the treatment area which had an unstructured organization, and the area was reduced. A little fibrous tissue was seen around it and a large number of inflammatory cells had infiltrated, showing an inflammatory cell reaction zone. In the treatment area of the

## Effect of Kupffer cells on residual tumor after cryoablation

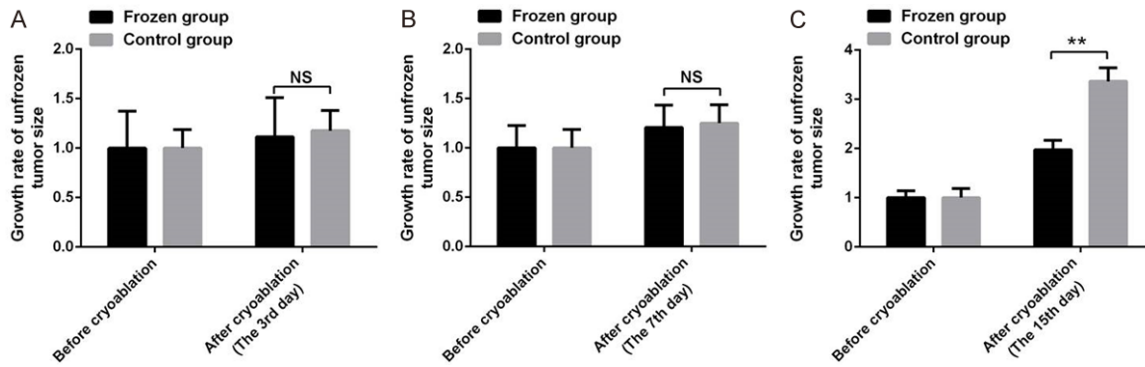


**Figure 1.** Unfrozen tumor in the frozen group grew slower on the 15th day after cryoablation. (A) On the 3rd day, (B) 7th day, and (C) 15th day, the size of frozen and control group tumor (cm) were detected before and after cryoablation. Considering that the tumor size before cryoablation in two groups was different, the tumor size before cryoablation was normalized to 1 by being divided by their average values respectively, and the tumor growth rates of unfrozen tumors after cryoablation in the frozen group and control group were compared. Data are presented as mean  $\pm$  SD (n=3), NS: No sense, \* $P$ <0.05, \*\* $P$ <0.01.

tumor not completely covered by the ice ball, the agglomerated new tumor cells could be seen around. The anti-CD68 immunohistochemical staining was strongly positive in the inflammatory reaction zone. The small nucleus-like round inflammatory cells were scattered among the unfrozen tumor cells too, and were significantly increased compared with that of 3 days after cryoablation. On the 15th day after cryoablation, there was a fibroplasia boundary around the necrotic area, with small nucleolus-like round inflammatory cells. Immunohistochemical staining showed cells with yellow-brown membrane or cytoplasm, mainly distributed around the necrotic area and being positive. Inflammatory cells were reduced among unfrozen tumor cells, and anti-CD68 immunohistochemical staining was negative. After 30 days, there were greyish nodules remained in the cryoablation area, which was hard and the liver had compensatory thickening. H&E staining suggested that there was an unstructured necrotic area among the nodules. The necrotic area was surrounded by a large amount of fibrous tissue. Inflammatory cells were reduced, and immunohistochemistry was weak positive (**Figure 2**).

### *Electron microscopic detection of KCs before and after cryoablation*

Before the cryoablation, the ultrastructure of the tumor cells and hepatocytes was clear. It could be seen that lymphocytes and KCs were scattered around the tumor cells, with folds and microvilli on the surface, and the endoplas-

mic reticulum, mitochondria, and phagosome were visible inside, with large cell nuclei. On the 3rd day after cryoablation, the structure of the cryoablation tissues were destroyed. The tumor cells and nucleus were blurred in outline and the chromatin was dissolved, which was replaced by scattered irregular cell clumps. The shape of the mitochondria became disintegrated and the mitochondrial substance was in lumpy. There were many well-formed white blood cells and KCs that devoured the tissue debris between the residual cell outlines around the cryoablation area. The number of organelles such as mitochondria and endoplasmic reticulum inside was increased, and the tissue debris was clearly visible. On the 7th day after cryoablation, the outlines of tumor cells and hepatocytes in the cryoablation area disappeared in a scattered, remnant state with disrupted membranous structures. We could see that the organelles disappeared, and mitochondria disintegrated. Meanwhile, the fibroblasts, well-formed white blood cells, and KCs that engulfed tissue debris were visible. Folds and microvilli in KCs were increased and rich in mitochondria, endoplasmic reticulum, phagocytic vesicles, and phagosomes. The cell nucleus was large, darkly stained, and the shape was irregular (**Figure 3**). At the 15th day, tumor cells and hepatocytes became cavitated and nuclear outlines had disappeared, showing debris and residues, with little difference between the central and near central regions. The inflammatory and fibrous reaction areas were further widened. The liver tissue in the

## Effect of Kupffer cells on residual tumor after cryoablation

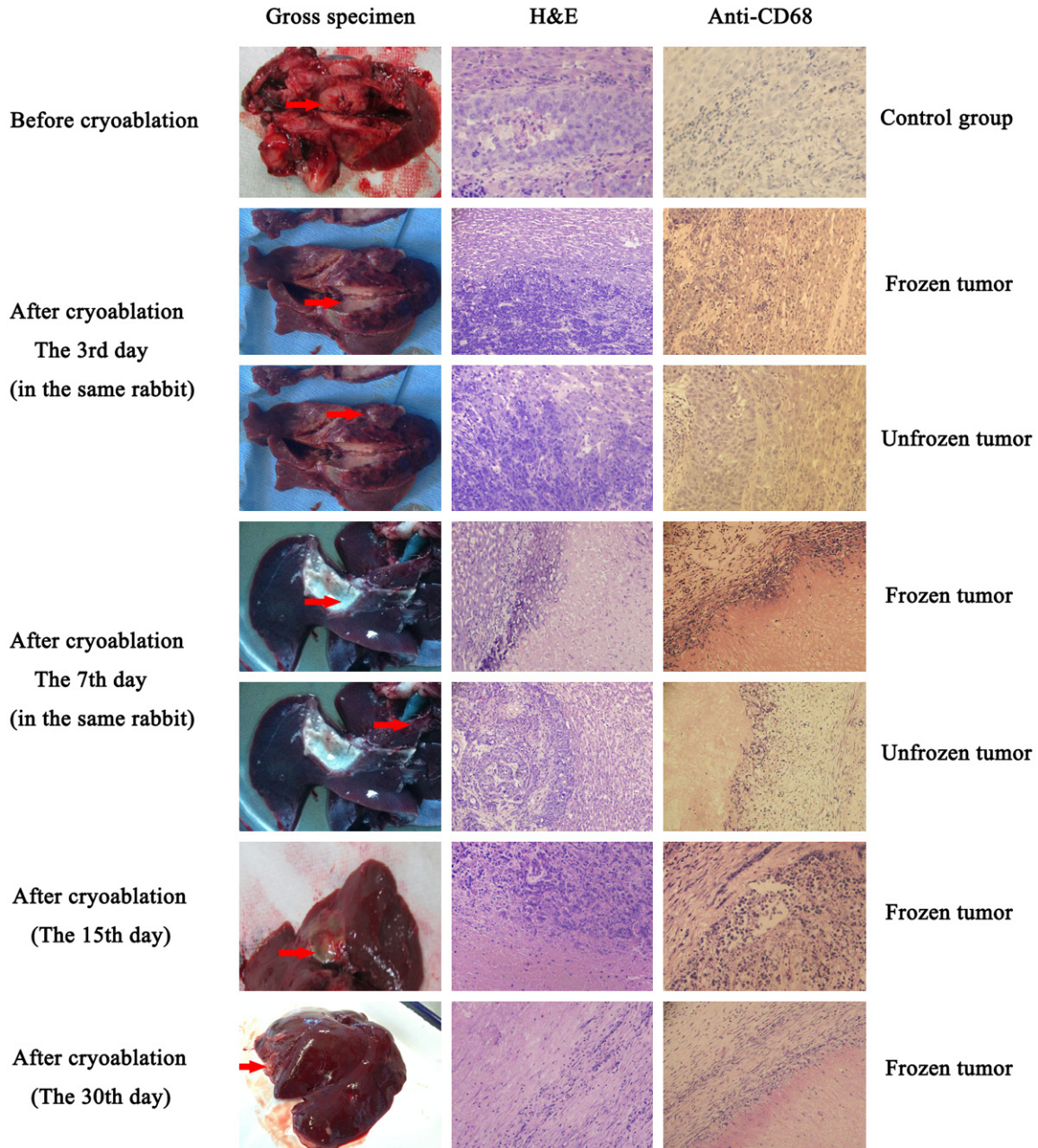


**Figure 2.** Comparison of the appearance and histology of the tumors before and after cryoablation. Gross appearance, H&E staining, and anti-CD68 immunohistochemical staining were recorded in the tumors before and after cryoablation (the 3rd day, 7th day, 15th day and 30th day). Because the anti-CD68 immunohistochemical staining of unfrozen tumor in the 15th and 30th day after cryoablation was negative, the results are not shown in the picture. The magnification was 400 $\times$ . “ $\rightarrow$ ” marks the representative location.

cryoablation area was in a lumpy mass and completely lost its tissue morphology.

*Counts of fragments engulfed in KCs under the electron microscope*

The phagocytic debris in KCs was about 0.5 cm away from cryoablation area and the unfro-

zen tumor lesions in the same animal were observed and compared with that before cryoablation. On the 3rd day after cryoablation, there was a significant difference in the debris amount in KCs when compared to that around the cryoablation area and that surrounding the unfrozen tumors,  $P < 0.05$ . On the 7th day after cryoablation, the average amount of phagocytic

## Effect of Kupffer cells on residual tumor after cryoablation

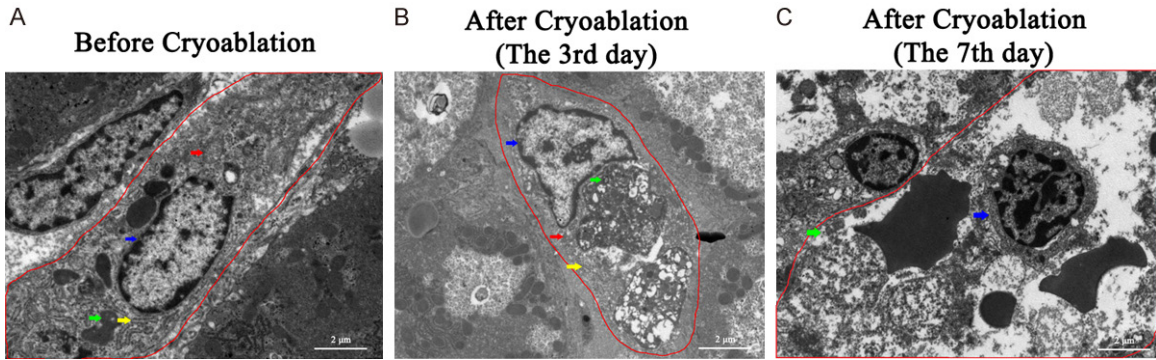


**Figure 3.** Electron microscopic detection of KCs before and after cryoablation. A. The shape of KCs was irregular, with folds and microvilli on the surface, and the endoplasmic reticulum, mitochondria and phagosome were visible inside, with large cell nucleus and irregular shapes, resembling binuclear due to folds. B. On the 3rd day after cryoablation, folds and microvilli of KCs increased. The number of organelles such as mitochondria and endoplasmic reticulum inside also increased. The tissue debris was clearly visible. The shape of the cell nucleus was irregular, such as crescent shape, with rather distinct form. C. On the 7th day after cryoablation, partial tissue debris was still clear while another part had been blurred. The cell nucleus was large, and darkly stained. The magnification was 5000 $\times$ . “ $\rightarrow$ ” marks mitochondria, “ $\rightarrow$ ” marks endoplasmic reticulum, “ $\rightarrow$ ” marks phagosome, and “ $\rightarrow$ ” marks cell nucleus.

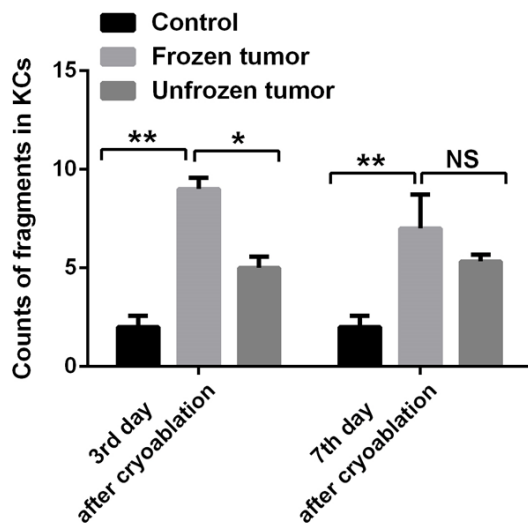


**Figure 4.** Counts of fragments engulfed by KCs under the electron microscope. On the 3rd day after cryoablation, there was a significant difference in the fragment number in KCs when compared with that around the cryoablation area (frozen tumor) and that surrounding the unfrozen tumors,  $P=0.031$ . On the 7th day after cryoablation, although the average number of phagocytic tissue fragments in KCs around cryoablation area was more than that of unfrozen tumors, there was no statistically significant difference,  $P=0.536$ . Also, the tissue debris in the KCs around the cryoablation lesions was significantly increased when compared with that before the cryoablation. Data are presented as mean  $\pm$  SD ( $n=3$ ), NS: No sense,  $*P<0.05$ ,  $**P<0.01$ .

tissue debris in KCs around the cryoablation area was more than that of unfrozen tumors,

but without significant difference,  $P>0.05$  (Figure 4).

### Discussion

As early as 1985, some scholars had found that the immune function of liver cancer patients was inhibited [25], including that cytokines such as IFN- $\gamma$  were also in a lower state [26]. Recent domestic scholars [27-29] have compared the cell immune function before and after cryoablation, and found that CD4+ and NK cells and dendritic cells (DCs) in patients with liver cancer before cryoablation were decreased; and after cryoablation, CD4+ and NK cells were significantly up-regulated, indicating that cryoablation could result in cellular immunological enhancement. Further studies [30] found that changes in inflammatory cells and Th1-dependent immune responses in tumor tissues could lead to enhanced activity of cancer-specific cytotoxic T lymphocytes. In our study, anti-CD68 monoclonal antibody was used to perform an immunohistochemical test and we found that the number of KCs was increased significantly after cryoablation around the tumor tissue, and immunohistochemical staining was strongly positive on the 3rd and 7th days after cryoablation. The small-round cells (mainly white blood cells) around the treatment area were also increased, forming a non-bacterial inflammatory response proliferative zone. With the extension of time, the number of fibroblasts around the treatment

## Effect of Kupffer cells on residual tumor after cryoablation

area gradually increased, and the numbers of KCs and small-round cells gradually decreased. For example, on the 15th and 30th days after cryoablation, immunohistochemical staining was significantly reduced. Baust *et al* [31] also reported the presence of inflammation found after cryoablation. Lymphocytes accumulated around the tumor tissues within 3 days, and the number of KCs peaked within 7 days and lasted for 15 days.

Some immune cells in the body can actively prevent tumorigenesis in a process and provide host defense against microbial infection and tumors, such as NK cells, NKT cells, and macrophage-lineage KCs [32, 33]. KCs produce IL-12 and TNF. IL-12 activates hepatic NK cells and NKT cells to produce IFN- $\gamma$ , which further activates hepatic T cells, in turn activating phagocytosis and cytokine production by KCs in a positive feedback loop [34]. Ablation treatment for liver cancer is a promising therapeutic strategy, and that ablation-induced immune activation serves an important role in suppressing cancer in animal models [35]. In this study, histology and immunohistochemistry were used to observe the change of unfrozen tumors as self-control after cryoablation. It has been found that: ① In the early stage after cryoablation (within 15 days), the size of unfrozen tumors did not change significantly. This may be related to too short a time interval, but inflammatory cell aggregation from histologic specimens could be seen around the unfrozen tumors [36]. Positive staining for KCs indicated that growth inhibition of the tumors could be obtained by stimulating the proliferation and activation of intrahepatic KCs after cryoablation and secreting inflammatory factors to induce inflammatory cell aggregation [37]. As early as 1972, Blackwood *et al* [38] found through animal experiments, that it was difficult to form tumors by transplantation of tumor cells in the abdominal cavity after cryoablation of carcinosarcoma. ② At 15 days of cryoablation, the growth of unfrozen tumors was statistically significantly restrained. While the inflammatory cells were gradually reduced compared with before, and immunohistochemical staining was negative, we could conclude that cryoablation could enhance the intrahepatic immune function in a certain period of time, including the aggregation of inflammatory cells and increased number and activities of KCs.

This had a certain impact on the unfrozen tumors in the same animal. It also seemed that the growth of unfrozen tumors was slower than the change of inflammatory cells, and the reduced growth speed of unfrozen tumors was probably caused by the accumulating effect of prior inflammatory cells. However, as time went on, the immune function changes caused by cryoablation gradually weakened, indicating that the inhibitory effect on the growth of unfrozen tumors would not last for a long time.

The main function of hepatic macrophages is to clear the portal circulation from foreign materials and pathogens using phagocytosis [39, 40]. In this study, the ultrastructure of KCs was observed by electron microscopy and the results showed that, when areas both around the cryoablation area and the untreated tumor area after cryoablation were compared with that before cryoablation, the KCs density was increased. Thus, the number of KCs was increased. Organelles such as endoplasmic reticulum and mitochondria became more abundant. Folds and microvilli on the surface increased [41, 42]. Mitochondria are important signaling organelles, and they dictate immunological fate and determine immune cell function [43]. Findings indicated the enhancement of KCs activity. The tissue debris inside was significantly increased compared with that of before cryoablation, which indicated that phagocytosis and scavenging action of KCs had been enhanced [44, 45]. The phagocytosis was not only enhanced in area around the cryoablation, but also was observed in the vicinity of unfrozen tumors in the same animal. On the 3rd and 7th day after cryoablation in this experiment, it was found that there was a significant difference between the debris in KCs around the frozen tumors and that in the control animals. Besides, debris in KCs around the unfrozen tumors was increased obviously on the 7th day, and there was no significant difference when comparing with the frozen tumors, indicating that the change in immune function after cryoablation was not limited to the area around the cryoablation, but it also attacked other tumors in the same animal body. KCs remove chemical compounds and dead or damaged cells, eliminate bacteria, and protect against invading tumor cells [46]. However, phagocytosis of KCs was only positive around senescent cells or cell debris, and

played a limited role in cell growth, which includes tumor cells [47]. This clarified that debris in KCs around the unfrozen tumors was significantly reduced, when compared with that surrounding the cryoablated area on the 3rd day after cryoablation.

### Conclusion

The inflammatory cell aggregation and the KC phagocytosis around the treatment area after cryoablation can cause further damage to the remaining tumor in the same body. This is essential for completely killing the tumor cells. The immune function changes after the cryoablation may have a certain inhibitory effect on the untreated tumor of the same animal body in early stages, but along with the decrease in inflammatory cells, it is not enough to control the growth of the tumor for a long time.

### Disclosure of conflict of interest

None.

**Address correspondence to:** Fengtao Yi, Department of Oncology, General Hospital of Central Theater Command of Chinese People's Liberation Army, No. 627 Wuluo Road, Wuchang District, Wuhan 430070, Hubei, P. R. China. E-mail: flzxyft@163.com

### References

- [1] Torre LA, Bray F, Siegel RL, Ferlay J, Lortet-Tieulent J and Jemal A. Global cancer statistics, 2012. *CA Cancer J Clin* 2015; 65: 87-108.
- [2] McGuire S. World Cancer Report 2014. Geneva, Switzerland: World Health Organization, International Agency for Research on Cancer, WHO Press, 2015. *Adv Nutr* 2016; 7: 418-419.
- [3] Katanoda K and Matsuda T. Five-year relative survival rate of liver cancer in the USA, Europe and Japan. *Jpn J Clin Oncol* 2014; 44: 302-303.
- [4] Lee JG, Kang CM, Park JS, Kim KS, Yoon DS, Choi JS, Lee WJ and Kim BR. The actual five-year survival rate of hepatocellular carcinoma patients after curative resection. *Yonsei Med J* 2006; 47: 105-112.
- [5] Bird HM and James Arnott MD. (aberdeen) 1797-1883: a pioneer in refrigeration analgesia. *Anesthesia* 1949; 4: 10-17.
- [6] Yi FT, Song HZ and Li J. Clinical application of ultrasound-guided Argon-Helium targeted ablation in treatment of liver tumor. *Chinese Journal of Ultrasonography* 2004; 13: 436-438.
- [7] Baust JM, Rabin Y, Polascik TJ, Santucci KL, Snyder KK, Van Buskirk RG and Baust JG. Defeating cancers' adaptive defensive strategies using thermal therapies: examining cancer's therapeutic resistance, ablative, and computational modeling strategies as a means for improving therapeutic outcome. *Technol Cancer Res Treat* 2018; 17: 1533033818762207.
- [8] Kato T, Iwasaki T, Uemura M, Nagahara A, Higashihara H, Osuga K, Ikeda Y, Kiyotani K, Park JH, Nonomura N and Nakamura Y. Characterization of the cryoablation-induced immune response in kidney cancer patients. *Oncoimmunology* 2017; 6: e1326441.
- [9] Ivanov S, Merlin J, Lee MKS, Murphy AJ and Guinamard RR. Biology and function of adipose tissue macrophages, dendritic cells and B cells. *Atherosclerosis* 2018; 271: 102-110.
- [10] Krenkel O and Tacke F. Liver macrophages in tissue homeostasis and disease. *Nat Rev Immunol* 2017; 17: 306-321.
- [11] Ritz T, Krenkel O and Tacke F. Dynamic plasticity of macrophage functions in diseased liver. *Cell Immunol* 2018; 330: 175-182.
- [12] Li P, He K, Li J, Liu Z and Gong J. The role of Kupffer cells in hepatic diseases. *Mol Immunol* 2017; 85: 222-229.
- [13] Wohlleber D and Knolle PA. The role of liver sinusoidal cells in local hepatic immune surveillance. *Clin Transl Immunology* 2016; 5: e117.
- [14] Yuan F, Zhang W, Mu D and Gong J. Kupffer cells in immune activation and tolerance toward HBV/HCV infection. *Adv Clin Exp Med* 2017; 26: 739-745.
- [15] Xu GJ, Liu JP, Ji Q, Wu JY, Wang ZJ, Li BL, Jiang H, Niu CY and Zhao ZG. Changes of erythrocyte rheology in rabbits with acute renal failure. *Zhongguo Ying Yong Sheng Li Xue Za Zhi* 2013; 29: 174-177.
- [16] Tanaka K, Maeda N, Osuga K, Higashi Y, Hayashi A, Hori Y, Kishimoto K, Morii E, Ohashi F and Tomiyama N. In vivo evaluation of irinotecan-loaded QuadraSphere microspheres for use in chemoembolization of VX2 liver tumors. *J Vasc Interv Radiol* 2014; 25: 1727-1735, e1721.
- [17] Gorman JR, Abrahamson J, Mordohovich D and Feldman M. Nonorganophilic, hematogenous dissemination in the presence of positive lymph nodes of a malignant tumor in rabbits. *Invasion Metastasis* 1984; 4 Suppl 1: 44-59.
- [18] Kuszyk BS, Boitnott JK, Choti MA, Bluemke DA, Sheth S, Magee CA, Horton KM, Eng J and Fishman EK. Local tumor recurrence following hepatic cryoablation: radiologic-histopathologic correlation in a rabbit model. *Radiology* 2000; 217: 477-486.
- [19] Takahashi Y, Izumi Y, Matsutani N, Dejima H, Nakayama T, Okamura R, Uehara H and

## Effect of Kupffer cells on residual tumor after cryoablation

- Kawamura M. Optimized magnitude of cryosurgery facilitating anti-tumor immunoreaction in a mouse model of Lewis lung cancer. *Cancer Immunol Immunother* 2016; 65: 973-982.
- [20] Guo WC, He XF, Li YH, Li ZH, Mei QL and Chen Y. The effect of sequential transcatheter arterial chemoembolization (TACE) and portal venous embolizations (PVE) vs. TACE or PVE alone on rabbit VX2 liver carcinoma and on liver regeneration. *Eur Rev Med Pharmacol Sci* 2016; 20: 3186-3193.
- [21] Claro F Jr, Morari J, Moreira LR, Sarian LO, Pinto GA, Velloso LA and Pinto-Neto AM. Unmanipulated native fat exposed to high-energy diet, but not autologous grafted fat by itself, may lead to overexpression of Ki67 and PAI-1. *Springerplus* 2015; 4: 279.
- [22] Huang CS, Zhai JM, Zhu XX, Cai JP, Chen W, Li JH and Yin XY. BTG2 is down-regulated and inhibits cancer stem cell-like features of side population cells in hepatocellular carcinoma. *Dig Dis Sci* 2017; 62: 3501-3510.
- [23] Balint IB, Vizsy L, Vargovics E, Farics A, Parti K and Simon E. Cryosclerosis. A forgotten endovenous procedure for treating the incompetence of the great saphenous vein. Short term results. *Int Angiol* 2014; 33: 547-552.
- [24] Zhang F, Yang XC, Jia XW, Tang XH, Wang Z and Wang ZQ. Von Willebrand factor and ADAMTS13 plasma in older patients with high CHA2DS2-VASc Score with and without atrial fibrillation. *Eur Rev Med Pharmacol Sci* 2017; 21: 4907-4912.
- [25] Gilbert JC, Onik GM, Hoddick WK and Rubinsky B. Real time ultrasonic monitoring of hepatic cryosurgery. *Cryobiology* 1985; 22: 319-330.
- [26] Sato M, Goto S, Kaneko R, Ito M, Sato S and Takeuchi S. Impaired production of Th1 cytokines and increased frequency of Th2 subsets in PBMC from advanced cancer patients. *Anti-cancer Res* 1998; 18: 3951-3955.
- [27] Huang M, Wang X and Bin H. Effect of transcatheter arterial chemoembolization combined with argon-helium cryosurgery system on the changes of NK cells and T cell subsets in peripheral blood of hepatocellular carcinoma patients. *Cell Biochem Biophys* 2015; 73: 787-792.
- [28] Si TG, Wang JP and Guo Z. Analysis of circulating regulatory T cells (CD4+CD25+CD127-) after cryosurgery in prostate cancer. *Asian J Androl* 2013; 15: 461-465.
- [29] Kasuya A, Ohta I and Tokura Y. Structural and immunological effects of skin cryoablation in a mouse model. *PLoS One* 2015; 10: e0123906.
- [30] Osada S, Yoshida K and Saji S. A novel strategy by cryoablation for advanced hepatoma. *Anti-cancer Res* 2009; 29: 5203-5209.
- [31] Baust JG, Gage AA, Bjerklund Johansen TE and Baust JM. Mechanisms of cryoablation: clinical consequences on malignant tumors. *Cryobiology* 2014; 68: 1-11.
- [32] Morvan MG and Lanier LL. NK cells and cancer: you can teach innate cells new tricks. *Nat Rev Cancer* 2016; 16: 7-19.
- [33] Waldhauer I and Steinle A. NK cells and cancer immunosurveillance. *Oncogene* 2008; 27: 5932-5943.
- [34] Seki S, Nakashima H, Nakashima M and Kinoshita M. Antitumor immunity produced by the liver Kupffer cells, NK cells, NKT cells, and CD8 CD122 T cells. *Clin Dev Immunol* 2011; 2011: 868345.
- [35] Mo Z, Lu H, Mo S, Fu X, Chang S and Yue J. Ultrasound-guided radiofrequency ablation enhances natural killer-mediated antitumor immunity against liver cancer. *Oncol Lett* 2018; 15: 7014-7020.
- [36] Glasgow SC, Kanakasabai S, Ramachandran S, Mohanakumar T and Chapman WC. Complement depletion enhances pulmonary inflammatory response after liver injury. *J Gastrointest Surg* 2006; 10: 357-364.
- [37] Luo M, Shao B, Nie W, Wei XW, Li YL, Wang BL, He ZY, Liang X, Ye TH and Wei YQ. Antitumor and adjuvant activity of lambda-carrageenan by stimulating immune response in cancer immunotherapy. *Sci Rep* 2015; 5: 11062.
- [38] Blackwood CE and Cooper IS. Response of experimental tumor systems to cryosurgery. *Cryobiology* 1972; 9: 508-515.
- [39] Naito M, Hasegawa G, Ebe Y and Yamamoto T. Differentiation and function of Kupffer cells. *Med Electron Microsc* 2004; 37: 16-28.
- [40] Benacerraf B, Sebestyen MM and Schlossman S. A quantitative study of the kinetics of blood clearance of P32-labelled *Escherichia coli* and *Staphylococci* by the reticuloendothelial system. *J Exp Med* 1959; 110: 27-48.
- [41] Warren A, Benseler V, Cogger VC, Bertolino P and Le Couteur DG. The impact of poloxamer 407 on the ultrastructure of the liver and evidence for clearance by extensive endothelial and kupffer cell endocytosis. *Toxicol Pathol* 2011; 39: 390-397.
- [42] Collier DS, Pain JA, Wight DG, Lovat P and Bailey ME. The Kupffer cell in experimental extrahepatic cholestasis in the rat—a light microscopy, immunohistochemical and electron microscopy study. *J Pathol* 1986; 150: 187-194.
- [43] Mehta MM, Weinberg SE and Chandel NS. Mitochondrial control of immunity: beyond ATP. *Nat Rev Immunol* 2017; 17: 608-620.
- [44] Miyazaki H, Sawada T, Kiyohira M, Yu Z, Nakamura K, Yasumoto Y, Kagawa Y, Ebrahimi M, Islam A, Sharifi K, Kawamura S, Kodama T, Ya-

## Effect of Kupffer cells on residual tumor after cryoablation

- mamoto Y, Adachi Y, Tokuda N, Terai S, Sakaida I, Ishikawa T and Owada Y. Fatty acid binding protein 7 regulates phagocytosis and cytokine production in Kupffer cells during liver injury. *Am J Pathol* 2014; 184: 2505-2515.
- [45] Corsaro C, Scalia M, Leotta N, Mondio F and Sichel G. Characterisation of Kupffer cells in some Amphibia. *J Anat* 2000; 196: 249-61.
- [46] Paschos KA, Majeed AW and Bird NC. Role of Kupffer cells in the outgrowth of colorectal cancer liver metastases. *Hepatol Res* 2010; 40: 83-94.
- [47] Krishnan V, Schaar B, Tallapragada S and Dorigo O. Tumor associated macrophages in gynecologic cancers. *Gynecol Oncol* 2018; 149: 205-213.